Non-linear attenuation of gravity wind waves*

OCEANOLOGIA, 20, 1985
PL ISSN 0078-3234

Non-linear wind waves
Pressure attenuation

ANDRZEJ NAGUSZEWSKI,
STANISŁAW MASSEL,
WOJCIECH TRAPP
Institute of Hydroengineering,
Polish Academy of Sciences,
Gdańsk-Oliwa

Manuscript received 5 July 1983, in final form 10 October 1983.

Abstract

The non-linear attenuation of the wave motion induced by wind is considered. From the collected experimental data is shown that the low frequencies are damping slower than it is given by a linear thoery. The opposite behaviour is observed in the high frequency range. The developed non-linear perturbation scheme offers a theoretical base for understanding of this unclassical attenuation mechanism.

1. Introduction

The dynamic motion of the sea surface, due to continuity of water masses, penetrates deeply into water. Penetration range depends strongly on the intensity of the surface motion and the respected frequency. Under the assumption that the observed surface geometry is a linear superposition of simple harmonic waves coming from various directions, the pressure damping of the particular components is described by well known classical formula [10]:

$$p(z) \sim \cosh k(z+h),$$

where:
- p – wave pressure;
- h – water depth;
- z – vertical coordinate of pressure measurement point, positive when upward;
- k – wave number related to wave frequency ω by the dispersion relation:

$$\omega^2 = g \cdot k \cdot \tanh(k \cdot h). \qquad (2)$$

* The investigations were carried out under the research programme MR.I. 15, coordinated by the Institute of Oceanology of the Polish Academy of Sciences.

The simplicity of attenuation factor is of the practical importance for the sea surface measuring procedure. Pressure type gauges therefore are extensively used in many locations throughout the world. The use of a pressure transducer for wave measurements present notable advantages in comparison with other systems. First of all, most systems are used on the surface, whereas a pressure transducer can be placed submerged, out of the way of being easily damaged. Moreover, it offers the precision which is quite satisfactory for the routine wave measurements. However, there is still a problem. It concerns the translation of information on wave pressure head variations into the concurrent surface wave heights.

Attempts to determine the validity of the classical attenuation law have been made in the past [1]. Previous experiments reported by Draper [9], Cypluchin [8], Bergan, Tørum and Traetteberg [2], Esteva and Harris [11], Cavaleri, Ewing and Smith [6], Grace [14] and Cavaleri [5] indicate that the deviations from the linear transmittance function are sometimes greater than 20%, depending on the frequency.

Moreover, in the monography published by Gluchovsky [13] (see also [10]), the empirical evidences for faster (than classical) attenuation of the separate, well noticeable, sea surface oscillations are collected. According to Gluchovski we have:

$$\gamma = \frac{\cosh k(z+h)}{\cosh kh} \cdot \exp\left\{-\left[kz - 5.5\left(\frac{z}{L}\right)^{0.8}\right]\right\}, \tag{3}$$

where: γ – averaged Gluchovski damping coefficient, L – wave length. Futher-

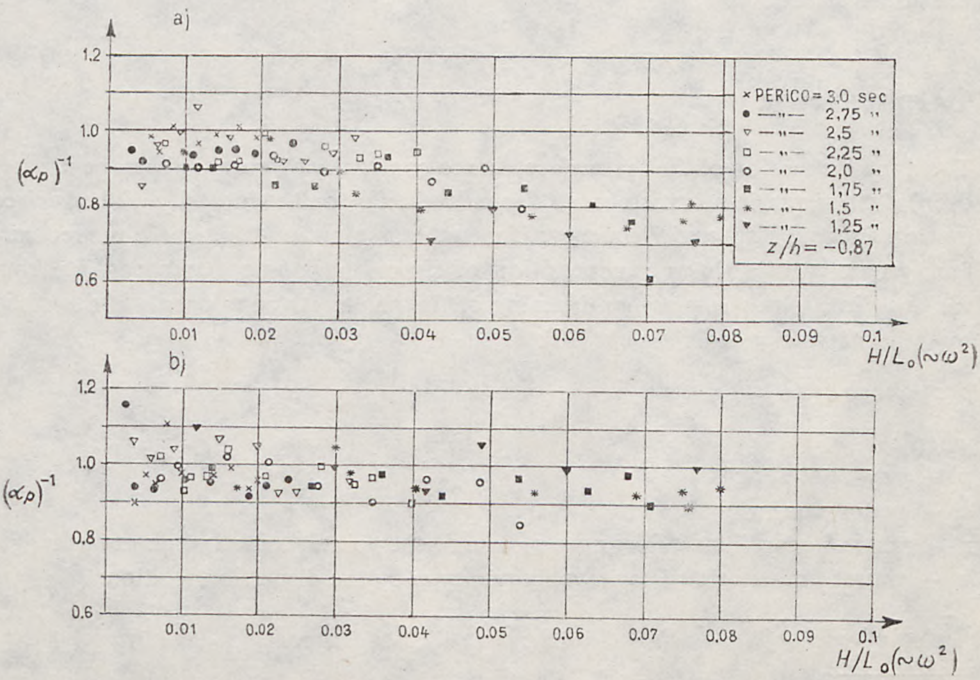

Fig. 1. Experimental and theoretical attenuation of wave pressure [2] a) according to linear theory; b) according to 5th order theory

more, the energy of the spectral component attenuates almost in accordance with the linear theory.

The review of the professional literature indicates [1, 12, 23, 27] that the discrepancies in the damping rate also for the orbital velocities were observed.

In this paper, some possible reasons for the discovered unclassical pressure damping are analyzed theoretically. The special efforts are made to demonstrate the importance of the non-linear mechanisms. Thus, a method correct to the second order in wave amplitude is applied for calculation of the non-linear damping coefficient α_p in the random wave field.

Using the theoretical results, the interpretation of the experiments is given. Moreover, the influence of other factors on the pressure attenuation rate is mentioned.

2. Non-linear attenuation function for wave pressure

The experiments carried out for the regular and irregular waves have shown [2] that transmittance function based on the non-linear wave theories predicts the wave attenuation much better than the linear one (Fig. 1). Particularly the application of the fifth order Stockes' approximation fits the experimental points quite satisfactorily. Therefore the conclusion that the non-linear mechanisms are responsible for the attenuation is well-founded.

In this chapter the corresponding non-linear theory up to the second order is developed using the perturbation method. It is assumed that all variables can be expanded as a convergent power series of a small parameter (proportional to the water – surface slope).

2.1 Problem formulation

We consider unrestricted water basin with constant water depth h. The waves are generated by wind stationary in time, as well as in space. If the effects of viscosity and turbulence can be regarded as small and the wave motion is irrotational, for the random velocity potential Φ and random sea surface ζ we have:

$$\Phi(\vec{x}, z, t) = \Phi^{(1)}(\vec{x}, z, t) + \Phi^{(2)}(\vec{x}, z, t) + \dots, \tag{4}$$

$$\zeta(\vec{x}, t) = \zeta^{(1)}(\vec{x}, t) + \zeta^{(2)}(\vec{x}, t) + \dots, \tag{5}$$

where: x, y – horizontal Cartesian co-ordinates with the orgin at the still water level.

The resulting boundary value problem is summarized as follows [28]:

$$\nabla^2\Phi = 0, \vec{u} = \nabla\Phi; \tag{6}$$

$$g\zeta+\frac{\partial\Phi}{\partial t}+\frac{1}{2}\vec{u}^2=0, \text{ where } z=0; \tag{7}$$

$$\frac{\partial\zeta}{\partial t}-\frac{\partial\Phi}{\partial z}+\frac{\partial\Phi}{\partial x}\cdot\frac{\partial\zeta}{\partial x}+\frac{\partial\Phi}{\partial y}\cdot\frac{\partial\zeta}{\partial y}=0, \quad \text{where } z=0; \tag{8}$$

$$\frac{\partial\Phi}{\partial z}=0, \quad \text{where } z=-h. \tag{9}$$

If we neglect the non-linear terms in (7) and (8), the solution of linear problem takes the form ([18, 24]):

$$\Phi^{(1)}(\vec{x},z,t)=\sum_{i=1}^{n}a_i\cdot\varphi_i^{(1)}(\vec{x},z,t), \tag{10a}$$

and

$$\zeta^{(1)}(\vec{x},t)=\sum_{i=1}^{n}a_i\cdot\zeta_i^{(1)}(\vec{x},t), \tag{10b}$$

where:

$$\varphi_i^{(1)}=\frac{g}{\omega_i}\cdot\frac{\cosh k_i(z+h)}{\cosh k_i h}\cdot\sin\psi_i; \quad \zeta_i^{(1)}=\cos\psi_i, \tag{11}$$

$$\psi_i^{(1)}=\vec{k}_i\cdot\vec{x}-\omega_i\cdot t+\varepsilon_i; \quad \vec{x}=(x,y), \tag{12}$$

$$\vec{k}_i=(k_i\cdot\cos\theta_i,\, k_i\cdot\sin\theta_i); \quad k_i=|\vec{k}_i|. \tag{13}$$

The amplitudes a_i and phases ε_i are chosen randomly, so that $a_i\cos\varepsilon_i$ and $a_i\sin\varepsilon_i$ are jointly normal, with ε_i uniformly distributed and:

$$\lim_{n\to\infty}\Big(\sum_{\omega<\omega_i<\omega+d\omega}\sigma_i^2\Big)=S_\zeta(\omega)\,d\omega+0\,(d\omega)^2, \tag{14}$$

where: σ_i – variance of sea surface elevation: $S_\zeta(\omega)$ – spectral density of wave energy.

Please note that in our model the amplitude a_i and frequency ω_i are associated with wave direction θ_i. Therefore, the directional wave characteristics is only partly taken into account.

The second order wave system is one that is forced by the linear system, *i.e.* all second order amplitudes and phases are related to the characteristics of the first order spectrum. In order to simplify the future algebra we assume the potential and sea surface ordinate of the second order in the forms:

$$\Phi^{(2)}(\vec{x},z,t)=\sum_{i=1}^{n}a_i^2\varphi_i^{(2)}(\vec{x},z,t)+\sum_{i=1}^{n-1}\sum_{j=i+1}^{n}a_i\cdot a_j\cdot\varphi_{i\varphi j}^{(2)}(\vec{x},z,t), \tag{15}$$

$$\zeta^{(2)}(\vec{x},t)=\sum_{i=1}^{n}a_i^2\cdot\zeta^{(2)}(\vec{x},t)+\sum_{i=1}^{n-1}\sum_{j=i+1}^{n}a_i\cdot a_j\cdot\zeta_{i\varphi j}^{(2)}(\vec{x},t). \tag{16}$$

First summation expresses the interaction of the spectral components with the same frequency, whereas the second double summation describes the result of the component interaction with different frequences. This case will be treated first.

2.2 Non-linear interaction of spectral components with different frequencies

The perturbation method yields the following equations set for the functions $\varphi_{ij}^{(2)}$ and $\zeta_{ij}^{(2)}$ in the form [17, 18]:

$$\nabla^2 \varphi_{ij}^{(2)}=0, \quad i=1,2,\ldots,n-1; \quad j=1,2,\ldots,n; \quad j>i; \tag{17}$$

$$g\cdot\zeta_{ij}^{(2)}+\frac{\partial\varphi_{ij}^{(2)}}{\partial t}=-\zeta_i^{(1)}\frac{\partial^2\varphi_j^{(1)}}{\partial z\partial t}-\zeta_j^{(1)}\varphi\frac{\partial^2\varphi_i^{(1)}}{\partial z\partial t}-\vec{u}_i^{(1)}\cdot\vec{u}_j^{(1)} \quad \text{at } z=0; \tag{18}$$

$$\frac{\partial\zeta_{ij}^{(2)}}{\partial t}-\frac{\partial\varphi_{ij}^{(2)}}{\partial z}=\zeta_i^{(1)}\frac{\partial^2\varphi_j^{(1)}}{\partial z^2}+\zeta_j^{(1)}\frac{\partial^2\varphi_i^{(1)}}{\partial z^2}-\left(\frac{\partial\varphi_i^{(1)}}{\partial x}\cdot\frac{\partial\zeta_j^{(1)}}{\partial x}+\frac{\partial\varphi_j^{(1)}}{\partial y}\cdot\frac{\partial\zeta_i^{(1)}}{\partial y}\right) \quad \text{at } z=0; \tag{19}$$

$$\frac{\partial^2\varphi_{ij}^{(2)}}{\partial t^2}+g\cdot\frac{\partial\varphi_{ij}^{(2)}}{\partial z}=-\zeta_i^{(1)}\cdot\frac{\partial}{\partial z}\left(\frac{\partial^2\varphi_j^{(1)}}{\partial t^2}+g\cdot\frac{\partial\varphi_j^{(1)}}{\partial z}\right)-$$

$$+\zeta_j^{(1)}\cdot\frac{\partial}{\partial z}\left(\frac{\partial^2\varphi_i^{(1)}}{\partial t^2}+g\cdot\frac{\partial\varphi_i^{(1)}}{\partial z}\right)-2\cdot\frac{\partial}{\partial t}(\vec{u}_i\vec{u}_j) \quad \text{at } z=0; \tag{20}$$

$$\frac{\partial\varphi_{ij}^{(2)}}{\partial z}=0 \quad \text{at } z=-h. \tag{21}$$

Substitution of (11) in (20) gives:

$$\frac{\partial^2\varphi_{ij}^{(2)}}{\partial t^2}+g\cdot\frac{\partial\varphi_{ij}^{(2)}}{\partial z}=-\frac{g^2k_i\varphi k_j}{\omega_i\varphi\omega_j}\cdot[\Pi_{ij}^{(+)}\cdot\sin(\psi_i-\psi_j)+\Pi_{ij}^{(-)}\sin(\psi_j-\psi_i)], \tag{22}$$

in which:

$$\Pi_{ij}^{(+)}=(\omega_i-\omega_j)[\cos\theta_{ij}-\tanh k_i h\cdot\tanh k_j h]+$$

$$+\frac{1}{2}\varphi\left[\frac{\omega_i\varphi k_j}{k_i}(1-\tanh^2 k_j h)+\frac{\omega_j\varphi k_i}{k_j}(1-\tanh^2 k_i h)\right]; \tag{23}$$

$$\Pi_{ij}^{(-)}=(\omega_i-\omega_j)[\cos\theta_{ij}+\tanh k_i h\cdot\tanh k_j h]+$$

$$+\frac{1}{2}\left[\frac{\omega_i\varphi k_j}{k_i}(1-\tanh^2 k_j h)-\frac{\omega_j k_i}{k_j}(1-\tanh^2 k_i h)\right]. \tag{24}$$

The solution of the differential equation (22) depends strongly on the character of the interactions involved. It is well known that for the second order solution only non-resonant interactions can be considered [22].
Therefore we obtain:

$$\varphi_{ij}^{(2)}=\frac{g^2k_ik_j}{\omega_i\omega_j}\left\{P_{ij}^{(+)}\cdot\frac{\cosh[|\vec{k}_i+\vec{k}_j|(z+h)]}{\cosh[|\vec{k}_i+\vec{k}_j|\cdot h]}\sin(\psi_i+\psi_j)+\right.$$

$$\left.+P_{ij}^{(-)}\frac{\cosh[|\vec{k}_j-\vec{k}_i|(z+h)]}{\cosh[|\vec{k}_j-\vec{k}_i|\cdot h]}\cdot\sin(\psi_j-\psi_i)\right\}, \tag{25}$$

where:

$$P_{ij}^{(+)}=\frac{\Pi_{ij}^{(+)}}{(\omega_i+\omega_j)^2-g\,|\vec{k}_i+\vec{k}_j|\cdot\tanh[|\vec{k}_i+\vec{k}_j|\cdot h]};$$

$$P_{ij}^{(-)}=\frac{\Pi_{ij}^{(-)}}{(\omega_i-\omega_j)^2-g\,|\vec{k}_i-\vec{k}_j|\tanh[|\vec{k}_j-\vec{k}_i|\cdot h]}; \tag{27}$$

and:

$$\zeta_{ij}^{(2)}=M_{ij}^{(+)}\cos(\psi_i+\psi_j)+M_{ij}^{(-)}\cos(\psi_i-\psi_j), \tag{28}$$

where:

$$M_{ij}^{(+)}=\frac{g\cdot k_i\cdot k_j}{\omega_i\cdot\omega_j}\left[(\omega_i+\omega_j)\cdot P_{ij}^{(+)}+\frac{1}{2}\cdot\left(\frac{\omega_i}{\omega_j}+\frac{\omega_j}{\omega_i}+1\right)\cdot\right.$$

$$\left.\cdot\tanh k_i h\cdot\tanh k_j h-\frac{1}{2}\cos\theta_{ij}\right]; \tag{29}$$

$$M_{ij}^{(-)}=\frac{gk_i\cdot k_j}{\omega_i\omega_j}\cdot\left[(\omega_j-\omega_i)\cdot P_{ij}^{(-)}+\frac{1}{2}\cdot\left(\frac{\omega_j}{\omega_i}+\frac{\omega_i}{\omega_j}-1\right)\cdot\right.$$

$$\left.\cdot\tanh k_i h\cdot\tanh k_j h-\frac{1}{2}\cos\theta_{ij}\right]. \tag{30}$$

The coefficients M_{ij} are symmetric, *i.e.* $M_{ij}=M_{ji}$.

In the special case when $h\to\infty$, $\varphi^{(2)}$ assumes the form [22]:

$$\varphi_{ij}^{(2)}=\frac{g^2k_ik_j}{\omega_i\omega_j}\left[\frac{(\omega_j-\omega_i)\cdot\cos^2\frac{1}{2}\theta_{ij}}{(\omega_j-\omega_i)^2-g|\vec{k}_j-\vec{k}_i|}\cdot e^{|\vec{k}_j-\vec{k}_i|\,z}\cdot\sin(\psi_j-\psi_i)+\right.$$

$$\left.-\frac{(\omega_i+\omega_j)\cdot\sin^2\frac{1}{2}\theta_{ij}}{(\omega_i+\omega_j)^2-g\,|\vec{k}_i+\vec{k}_j|}\cdot e^{|\vec{k}_i-\vec{k}_j|\,z}\cdot\sin(\psi_i+\psi_j)\right], \tag{31}$$

what is in agreement with Longuet-Higgins' result [18].

2.3 Non-linear interaction of spectral components with the same frequencies

When the frequencies ω_i and ω_j are identical, the interaction mechanism creates the well-known Stokes' component. Thus, the derivation of the formulas for the potential $\varphi^{(2)}$ and surface elevation $\zeta^{(2)}$ will be omitted here. We summarize only the final expressions as follows:

$$\varphi_i^{(2)} = \frac{g^2 k_i^2}{2\omega_i} \cdot P_{ii}^{(+)} \cdot \frac{\cosh[2k_i(z+h)]}{\cosh(2k_i h)} \cdot \sin 2\psi_i, \tag{32}$$

where:

$$P_{ii}^{(+)} = \frac{3}{4} \cdot \frac{\omega_i}{gk_i} \cdot \frac{\cosh 2k_i h}{\sinh^3 \cdot k_i \cdot h \cdot \cosh k_i h}; \quad P_{ii}^{(-)} = 0, \tag{33}$$

and:

$$\zeta_i^{(2)} = \tfrac{1}{2}[M_{ii}^{(+)} \cdot \cos 2\psi_i + M_{ii}^{(-)}], \tag{34}$$

in which:

$$M_{ii}^{(+)} = \frac{gk_i^2}{\omega_i^2} \cdot \frac{1 + 2 \cdot \cosh^2 k_i h}{2 \cdot \sinh k_i h}, \tag{35}$$

$$M_{ii}^{(-)} = -\frac{gk_i^2}{\omega_i^2} \cdot \frac{1}{2 \cdot \cosh^2 k_i h}. \tag{36}$$

The term $\frac{1}{2} \cdot M_{ii}^{(-)}$ describes only small departure of the mean water level from the initial position and it will be neglected below due to its nonperiodic behaviour.

It is clear that the final form of the second order velocity potential $\phi^{(2)}$ obeys the summation of (25) and (32) according to equation (15). These results can be easily compared with other forms developed by Krylov, Strekalov and Cypluchin [17], Bitner-Gregersen [4], and Sharma and Dean [25].

2.4 Autocorrelation and spectral functions for sea surface elevation

Since we have $\zeta = \zeta^{(1)} + \zeta^{(2)}$ by equations (11), (28) and (34), we can find the energy spectrum of a homogeneous stationary surface by first forming the autocorrelation function and taking its Fourier Transform in the usual way. We have:

$$K_\zeta(\tau) = \overline{\zeta(t) \cdot \zeta(t+\tau)} = \overline{\zeta^{(1)}(t) \cdot \zeta^{(1)}(t+\tau)} + \overline{\zeta^{(1)}(t) \cdot \zeta^{(2)}(t+\tau)} +$$

$$+ \overline{\zeta^{(2)}(t) \cdot \zeta^{(1)}(t+\tau)} + \overline{\zeta^{(2)}(t) \cdot \zeta^{(2)}(t+\tau)}. \tag{37}$$

The overbar denotes the averaging in the stochastic sense. Inspection of the equation (37) indicates that the particular terms are essentially second, third and fourth moments.

We will assume that the linear approximation to the sea surface $\zeta^{(1)}(t)$ and its linear potential function $\phi^{(1)}$ are Gaussian. However, the second order sea surface $\zeta^{(2)}$ can not be Gaussian, or the essential non-linearity is lost.
Since this is a perturbation analysis, the effect of M_{ij} is to make a small correction on the Gaussian probability, we can use the pseudo-Gaussian hypotesis that the third

and fourth moments will be related substantially as they are for the Gaussian case, *i.e.*:

$$\overline{\zeta^{(1)}(t)\cdot\zeta^{(2)}(t+\tau)}\approx\overline{\zeta^{(2)}(t)\cdot\zeta^{(1)}(t+\tau)}\approx 0, \tag{38}$$

while the first term in (37) gives

$$\overline{\zeta^{(1)}(t)\cdot\zeta^{(1)}(t+\tau)}=\sum_{i=1}^{n}\sum_{j=1}^{n}\overline{a_i\cdot a_j\cdot\cos\psi_i\cos(\psi_j-\omega_j\cdot\tau)}. \tag{39a}$$

Using the assumption on the stationary process, (39a) becomes ([16]):

$$\overline{\zeta^{(1)}(t)\cdot\zeta^{(1)}(t+\tau)}=\sum_{i=1}^{n}S_\zeta^{(1)}(\omega_i)\cdot\cos(\omega_i\cdot\tau)\cdot\Delta\omega. \tag{39b}$$

The fourth moment for the variables $u_j(j=1,2,3,4)$ can be related to the second one by [16]:

$$\overline{u_1\cdot u_2\cdot u_3\cdot u_4}=\overline{u_1\cdot u_2}\cdot\overline{u_3\cdot u_4}+\overline{u_1\cdot u_3}\cdot\overline{u_2\cdot u_4}+\overline{u_1\cdot u_4}\cdot\overline{u_2\cdot u_3}. \tag{40}$$

Equation (41) is essentially the Millionshthikov hypotesis, well known in the turbulence.

Substitution (38), (40) and (41) into (37) gives

$$K(\tau)=\sum_{i=1}^{n}S_\zeta^{(1)}\cdot\cos(\omega_i\tau)\cdot\Delta\omega+\{\sum_{i=1}^{n}M_{ii}^{(+)^2}\cdot S_{\zeta_i}^{(1)}\cdot\cos(2\omega_i\tau)+$$

$$+2\sum_{i=1}^{n-1}\sum_{j=i+1}^{n}[M_{ij}^{(+)^2}\cdot\cos((\omega_i+\omega_j)\cdot\tau)+M_{ij}^{(-)^2}\cdot\cos((\omega_j\omega_i)\cdot\tau)\cdot S_{\zeta_i}^{(1)}\cdot S_{\zeta_j}^{(1)}\}\cdot(\Delta\omega)^2 \tag{41}$$

The Fourier transformation of (42) yields the spectral function in the form:

$$S_{\zeta_k}(\omega_k)=S_{\zeta_k}^{(1)}+M_{ll}^{(+)^2}\cdot S_{\zeta_l}^{(1)^2}\cdot\Delta\omega+2\sum_{i=1}^{i=T}M_{i,k-1}^{(+)^2}\cdot S_{\zeta_i}^{(1)}\cdot S_{\zeta_{k-i}}^{(1)}\cdot\Delta\omega+$$

$$+2\sum_{i=1}^{i=T^{(-)}}M_{i,k+i}^{(-)^2}\cdot S_{\zeta_i}^{(1)}\cdot S_{\zeta_{k+i}}^{(1)}\Delta\omega, \tag{42}$$

where: $T^{(+)}=\text{Entier}\left(\frac{k-1}{2}\right)$; $T^{(-)}=n-k$; $k\leqslant n-1$. The term $M_{l,l}^{(+)}$ is applied only for even k ($l=k/2$). Expression (42) presents the non-linear spectrum for surface waves when second order terms are taken into account.

2.5 Autocorrelation and spectral functions for wave pressure

The perturbation method yields the following expressions for the wave-induced pressure (for simplicity $\vec{x}=0$) [28]:

$$p(z,t)=p^{(1)}(z,t)+p^{(2)}(z,t), \tag{43}$$

where:

$$p^{(1)}(z,t)=-p\frac{\partial\Phi^{(1)}}{\partial t}, \tag{44}$$

and

$$p^{(2)}(z,t)=-\rho\left\{\frac{\partial\Phi^{(2)}}{\partial t}+\frac{1}{2}\left[\left(\frac{\partial\Phi^{(1)}}{\partial x}\right)^2+\left(\frac{\partial\Phi^{(1)}}{\partial y}\right)^2+\left(\frac{\partial\Phi^{(1)}}{\partial z}\right)^2\right]\right\}. \tag{45}$$

Substitution of (11), (25) and (32) into (44) and (45) gives:

$$p^{(1)}(z,t)=\sum_{i=1}^{n}a_i\cdot p_i^{(1)}(z,t), \tag{46}$$

$$p_i^{(1)}(z,t)=\rho g\cdot C_i(z)\cdot\cos\psi_i;\qquad C_i(z)=\frac{\cosh k_i(z+h)}{\cosh k_i\cdot h}, \tag{47}$$

and:

$$p^{(2)}(z,t)=\sum_{i=1}^{n}a_i^2\cdot p_i^{(2)}(z,t)+\sum_{i=1}^{n-1}\sum_{j=i+1}^{n}a_i\cdot a_j\cdot p_{ij}^{(2)}(z,t), \tag{48}$$

in which:

$$p_i^{(2)}(z,t)=\tfrac{1}{2}\rho g\cdot[N_{ii}^{(+)}\cdot\cos 2\psi_i+N_{ii}^{(-)}], \tag{49}$$

$$p_{ij}^{(2)}(z,t)=\rho g\,[N_{ij}^{(+)}\cdot\cos(\psi_i+\psi_j)+N_{ij}^{(-)}\cdot\cos(\psi_j-\psi_i)], \tag{50}$$

$$N_{ij}^{(+)}=\frac{gk_ik_j}{\omega_i\omega_j}\cdot\left\{\frac{(1-\cos\theta_{ij})\cdot\cosh[(k_i+k_j)(z+h)]}{4\cdot\cosh k_i\cdot h\cdot\cosh k_j h}-\right.$$
$$\left.+\frac{(1+\cos\theta_{ij})\cdot\cosh[(k_j-k_i)(z+h)]}{4\cosh k_i h\cdot\cosh k_j h}+(\omega_i+\omega_j)\cdot P_{ij}^{(+)}\cdot\frac{\cosh[|\vec{k}_i+\vec{k}_j|(z+h)]}{\cosh[|\vec{k}_i+\vec{k}_j|\cdot h]}\right\}, \tag{51}$$

$$N_{ij}^{(-)}=\frac{gk_ik_j}{\omega_i\omega_j}\cdot\left\{\frac{(1+\cos\theta_{ij})\cdot\cosh[(k_i-k_j)(z+h)]}{4\cdot\cosh k_i h\cdot\cosh k_j h}+\right.$$
$$\left.+\frac{(1+\cos\theta_{ij})\cdot\cosh[(k_j-k_i)(z+h)]}{4\cosh k_i h\cdot\cosh k_j h}+(\omega_j-\omega_i)\cdot P_{ij}^{(-)}\frac{\cosh[|k_j-k_i|(z+h)]}{\cosh[|\vec{k}_j-\vec{k}_i|\cdot h]}\right\}. \tag{52}$$

The corresponding spectral function for the wave pressure takes the form:

$$\left(\frac{1}{\rho g}\right)^2 S_{p_k}=C_k^2\cdot S_{\zeta_k}^{(1)}+N_{ll}^{(+)^2}\cdot S_{\zeta_k}^{(1)^2}\cdot\Delta\omega+2\cdot\sum_{i=1}^{i=T(+)}N_{i,k-i}^{(+)^2}\cdot S_{\zeta_i}^{(1)}\cdot S_{\zeta_{k-i}}^{(1)}\cdot\Delta\omega+$$
$$+2\sum_{i=1}^{i=T(-)}N_{i,k+i}^{(-)^2}S_{\zeta_i}^{(1)}S_{\zeta_{k+i}}^{(1)}\Delta\omega. \tag{53}$$

It should be noted that the non-linear pressure spectrum depends on the directional spreading of the surface wave energy, whereas the linear spectrum is quite independent on wave direction.

Let us now assume that $\varphi_{ij}=0$, *i.e.* all spectral components propagate in the same direction. Therefore equations (51) and (52) become:

$$N_{ij}^{(+)}=\frac{gk_ik_j}{\omega_i\omega_j}\left\{-\frac{\cos h[(k_j-k_i)(z+h)]}{2\cos hk_ih\cdot\cos hk_jh}+(\omega_i+\omega_j)P_{ij}^{(+)}\frac{\cos h[(k_i+k_j)(z+h)]}{\cos h[(k_i+k_j)h]}\right\}, \quad (54)$$

$$N_{ij}^{(-)}=\frac{gk_ik_j}{\omega_i\omega_j}\left\{-\frac{\cos h[(k_i+k_j)(z+h)]}{2\cos hk_ih\cdot\cos hk_jh}+(\omega_j-\omega_i)P_{ij}^{(-)}\frac{\cos h[(k_j-k_i)(z+h)]}{\cos h[(k_j-k_i)h]}\right\}. \quad (55)$$

The coefficients N_{ij} have quite unexpected forms. For example, $N_{ij}^{(+)}$ which corresponds to the sum of frequencies $(\omega_i+\omega_j)$ depends not only on the classical term $\sim\cos h[(k_i+k_j)(z+h)]$ but also on term $\sim\cos h[(k_j-k_i)(z+h)]$. The decaying (with depth) of the last term is much slower than classical one. In the special case $\omega_i=\omega_j$, the last term will be constant with depth, indeed. In the same way we can argue that the term $\sim\cos h[(k_i+k_j)(z+h)]$ in the coefficient $N_{ij}^{(-)}$ decays faster than it comes from the linear theory. We use both conclusions in the following section extensively.

2.6 Non-linear attenuation of wave pressure with depth

Let us define the non-dimensional decaying function $Z^{(p)}(\omega_k, z)$ in the form:

$$Z^{(P)}(\omega_k, z)=\left\{\frac{(\rho g)^{-2}S_{pk}(\omega_k, z)}{S_{\zeta_k}(\omega)}\right\}^{\frac{1}{2}}. \quad (56)$$

After substituting (42) and (53) into (56) we get the non-linear decaying function $Z_{nl}^{(p)}(\omega_k, z)$ in the form:

$$Z_{nl}^{(P)}(\omega_k, z)=C_k(z)\left\{1.0+\left(\frac{N_{ll}^{(+)}}{C_k}\right)^2\frac{S_{\zeta_l}^{(1)}}{S_{\zeta_k}^{(1)}}\Delta\omega+2\left[\sum_{i=1}^{i=T(+)}\left(\frac{N_{i,k-i}}{C_k}\right)^2\frac{S_{\zeta_i}^{(1)}S_{\zeta_{k-i}}^{(1)}}{S_{\zeta_k}^{(1)}}\Delta\omega+\right.\right.$$
$$\left.\left.+\sum_{i=1}^{i=T(-)}\left(\frac{N_{i,k+i}^{(-)}}{C_k}\right)^2\frac{S_{\zeta_i}^{(1)}S_{\zeta_{k+i}}^{(1)}}{S_{\zeta_k}^{(1)}}\Delta\omega\right]\right\}:\left\{1.0+M_{ll}^{(+)2}\frac{S_{\zeta_l}^{(1)}}{S_{\zeta_k}^{(1)}}\Delta\omega+\right.$$
$$\left.+2\left[\sum_{i=1}^{i=T(+)}M_{i,k-i}^{(+)2}\frac{S_{\zeta_i}^{(1)}S_{\zeta_{k-i}}^{(1)}}{S_{\zeta_k}^{(1)}}\Delta\omega+\sum_{i=1}^{i=T(-)}M_{i,k+i}^{(-)2}\frac{S_{\zeta_i}^{(1)}S_{\zeta_{k+i}}}{S_{\zeta_k}^{(1)}}\Delta\omega\right]\right\}. \quad (47)$$

When the non-linear interaction is neglected, equation (5*b*) yields:

$$Z_l^{(P)}(\omega_k, z)=C_k(z). \quad (58)$$

Now, we define the pressure attenuation coefficient α_p as a rate of (57) and (58), *i.e.*:

$$\alpha_p(\omega_k, z)=Z_{nl}^{(P)}(\omega_k, z)/Z_l^{(P)}(\omega_k, z). \quad (59)$$

Therefore, if $\alpha_p(\omega_k, z)>0$ for given frequency ω_k, the non-linear pressure decaying is weaker than linear one. On the contrary, if $\alpha_p(\omega_k, z)<0$, the pressure decays faster than in the linear case. The identity $\alpha_p\equiv 1.0$ reflects the linear attenuation (see also [3]).

In the chapter 2.5, in the coefficient $N_{ij}^{(+)}$ (higher frequencies) we have detected terms decaying slowly. Thus, in this frequency range, the coefficient α_p should be somewhat greater than one. In the low frequency range it should be smaller than one, due to similar arguments. Experiments carried out recently [5, 14] seem to confirm these conclusions.

It should be pointed out that the non-linear attenuation coefficient α_u for the orbital velocities can be obtained in the similar way. However, the decaying terms in the high frequency range $(\omega_i+\omega_j)$ are proportional to the $\cosh[(k_i+k_j)(z+h)]$. On the contrary, for the low frequency, the velocities are decaying according to $\cosh[(k_i-k_j)(z+h)]$. Thus, they reflect the linear-like behaviour in all frequency range. In general, the damping coefficients $\alpha_p(\omega)$ or $\alpha_u(\omega)$ depend not only on the form of hiperbolic functions but also on the values of parameters N_{ij} and M_{ij} as well as on the shape of $S_\xi^{(1)}$ spectrum. Therefore, the final conclusions may be withdrawn only after detailed numerical calculations carried out for each particular case.

3. Experimental data and numerical calculations

We now summarize the data available on deterministic and stochastic correlations between surface wave heights and pressure head variations through 1982. Some of the data sources are listed in the **References**. Although the data were scattered, the general trend was for the empirical damping coefficient α to increase through unity with increasing wave frequency.

Draper [9] reported that waves in relatively deep water obey the classical hydrodynamical theory, whereas waves in shallow water may produce pressure on the sea bed almost 20% less than that suggested by the theory. As usually the waves in shallow water are relatively long ones. Thus, from theory given above we conclude that the coefficient α_p should be smaller than 1, what was observed precisely.

According to [8], the decaying of the well-defined particular oscillations in the deep sea is faster than predicted by linear theory for periods 4 - 10 s. This conclusion was conformed by Gluchovski [13]. In the Figure 2 the comparison of the empirical decaying coefficient and theoretical one based on the linear theory, is given. The faster attenuation is observed in the deep (Fig. 2a) as well as in the shallow water (Fig. 2b). The analytical formula (3), proposed by Gluchovski, corresponds to the curve which fits the experimental data in the best possible way. With respect to the spectral component attenuation, Gluchovski argues that the attenuation is in accordance with linear theory.

It is in some contradiction with Bergan, Tørum and Traetteberg experiments [2]. The experiments were made in a wave channel with a water depth of 1 m and for periods from 1.25 to 3 s. The pressure was measured at the point submerged 0.87 m under water. Figure 1 shows comparisons of pressure measured by the pressure gauge and pressure calculated from wave heights using the linear wave theory (Fig. 1a). In the same figure a similar comparison with the fifth order wave theory is also given (Fig. 1b); there is a fair agreement between measured pressures and pressures calculated according to the fifth order wave theory, indicating that the influence of the non-linearities on the pressure decaying is substantial and can not

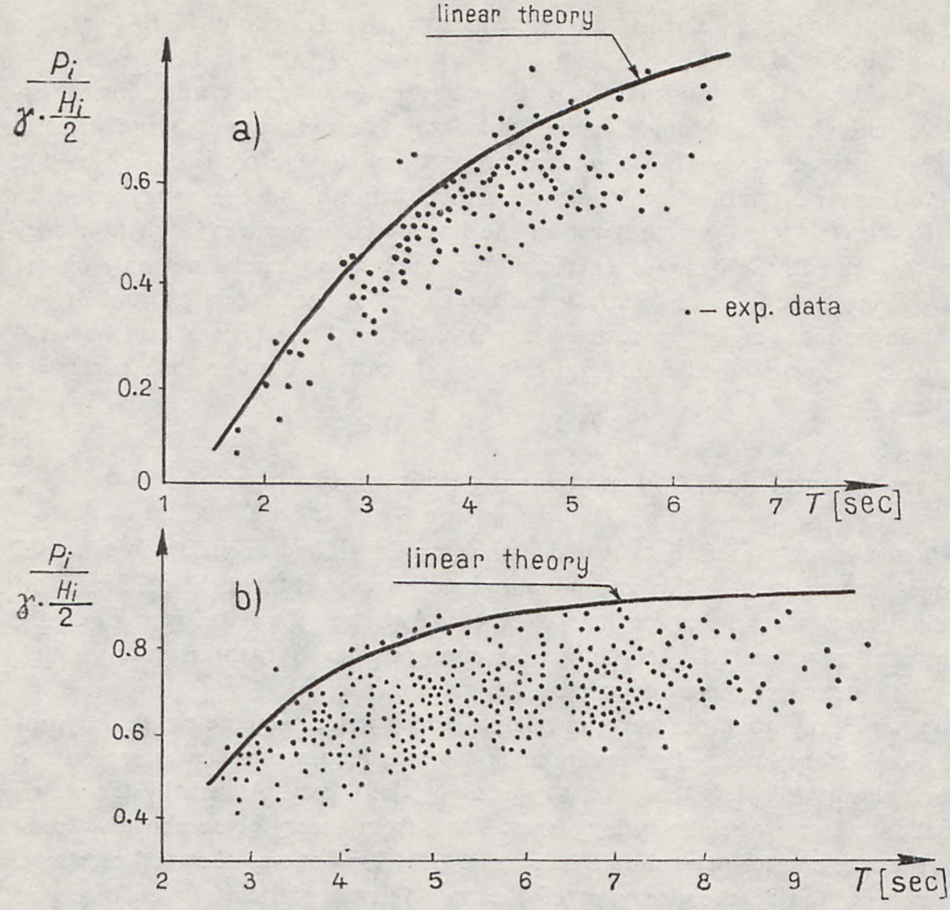

Fig. 2. Attenuation of particular sea surface oscillations, [13]; a) deep water; b) shallow water

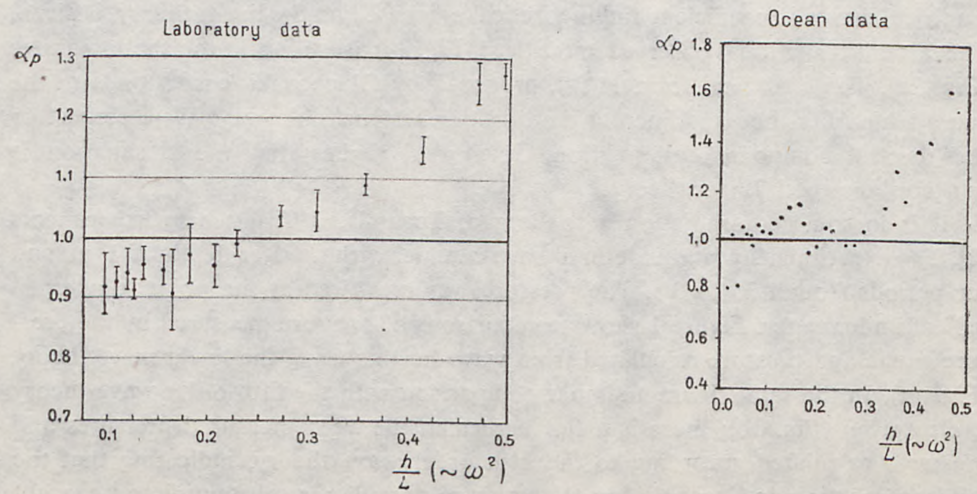

Fig. 3. Experimental damping coefficient α_p for laboratory and ocean data, [14]

be omitted. Also the spectral energy at a given point and for the higher frequencies is in general greater than that coming from the linear transmittance function.

The similar comparison was made by Esteva and Harris [11]. Two pressure gauges were involved in this work. One pressure sensor was immediately above the bottom, with the other one 1.7 m above it. During experiments the water depth was 4.7 m.

For the lower gauge, $\alpha_p(\omega)$ increased from about ~ 0.95 at a frequency of approximately 0.43 rd/s to ~ 1.05 for $\omega \sim 2$ rd/s. The upper gauge showed α_p values consistently closer to unity.

In the paper [14], both field and laboratory data are employed. The field data were taken in the ocean off Honolulu, in 11.3 m of water, and involved swell with periods from 12 to 17 s. The laboratory data were taken for water depths of 2.9 and 3.5 m and involved periods from 2 to 6 s. According to [14], the linear theory can be used to predict individual surface wave heights from pressure variations at, or near, the sea bed as long as an empirical correction factor is included. His empirical damping coefficient α is smaller than unity for small ratios of water depth to wave length (or for small frequencies) and greater than unity for larger values of this parameter (or for high frequencies) – see Figure 3. Thus, it agrees qualitatively with the prediction by the non-linear theory given above.

Recently Cavaleri, Ewing, Smith [6] published the results of an accurate experiment on an oceanographic tower. They found that generally waves attenuate in the different way than it is predicted by the linear theory, *i.e.* α_p can be smaller or greater than 1. The α_p coefficient shows approximately a linear dependence on frequency ω and the slope of this line depends on the depth of the transducer. The α_p value for some of the records has been plotted against frequency in Figure 4 [5].

The similar effect was observed for the pore pressure attenuation in the sandy sea bed [20]. For example, in Figure 5 the dependence of empirical coefficient α_p on the frequency is shown. The pressure gauge was installed 0.5 m under the sea bed; water depth was about 7.0 m. Again, the deviations from the linear attenuation for low and high frequency can be easily detected.

Let us consider the numerical calculation of the attenuation coefficient α_p using the formulas developed above. But there is still some problem. The coefficient α_p depends strongly on the linear frequency spectrum $S_\zeta^{(1)}$. In fact, it is unkown function because the spectra available in literature are usually the analytical expressions of the curves which fit the experimental data in the best possible manner. Moreover, it should be pointed out that the experimental data reflect the total superposition of the linear and non-linear phenomena in the wave motion. Thus, the linear spectrum $S_\zeta^{(1)}$ must be calculated from given experimental spectrum using the special numerical procedures. Two such procedures were developed recently by Chybicki and Naguszewski and for the details we address the readers to [8]. Therefore, the problem of separation of a given spectrum on linear and non-linear parts will be omitted here. In Figure 6, the result of spectrum separation for the record taken in the shallow water is shown, where we demonstrate the importance of the nonlinearities in the various frequency bands. If we subtract the non-linear part of

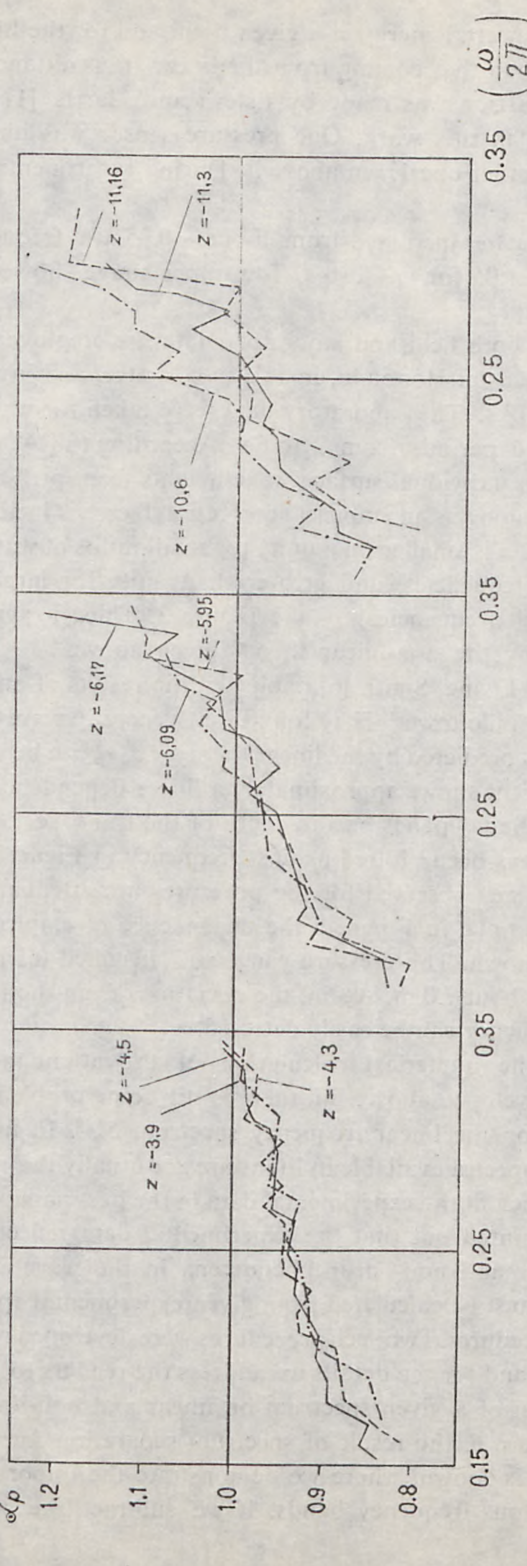

Fig. 4. Empirical coefficient α_p, [5]

spectrum from experimental one, we get the $S_\zeta^{(1)}$ function. Now, the pressure spectrum $S_p(\omega)$ and attenuation coefficient α_p can be calculated from formulas developed in chapter 2. Figure 7 illustrates the frequency dependence of the coefficient α_p for the same record as in Figure 6. In the basic energetic part of the spectrum coefficient α_p is very close to 1 and it is increasing rapidly when $\omega > 3\omega_p$. Therefore, the linear α_p describes correctly the pressure attenuation in the frequency range $\omega < 2\omega_p$ for the wave record under consideration. In general however, it is not ture. Many numerical experiments carried out by authors indicate that $\alpha_p(\omega)$ is strongly depending on the energy level in the low frequency range. The following example (see also [3]) demonstrates that fact very clearly. Let us consider the wind-induced waves characterized by JONSWAP spectrum ($T_p = 4$ s; $H_s = 2.3$ m, $\gamma_1 = 5$). Water depth is 12 m and pressure is measured on the sea bottom. The ordinates of JONSWAP spectrum are listed below:

No.	ω [rd/s]	S_ζ[m²·s]	No.	ω [rd/s]	S_ζ[m²·s]
1	0.157	0.0000	10	1.571	0.2350
2	0.314	0.0000	11	1.728	0.2170
3	0.471	0.0000	12	1.885	0.050
4	0.628	0.0000	13	2.042	0.0286
5	0.785	1.08E-8	14	2.199	0.0221
6	0.942	0.00014	15	2.356	0.0169
7	1.099	0.0054	16	2.513	0.0129
8	1.257	0.0237	17	2.670	0.0099
9	1.414	0.0830	18	2.827	0.0077

The resulting coefficient α_p is plotted in Figure 8 (solid line with circles). It can be seen that the α_p departure from the linear value 1 is rather large, specially in the frequency range outside of pik frequency. For the lower frequencies α_p is much smaller than 1 and in the high frequency range it becomes higher than 1. Now we modify slightly the three first spectrum ordinates inserting zero instead, identical ordinates equal to $S(\omega) = 0.02$. Physically it means that we consider the energy given by low--frequency oscillations of surf beats or edge waves type. In Figure 8 the effect of spectrum modification is illustrated by the broken line. The resulting α_p curve differs now from the linear constant value not only at the very low or very high frequencies but also in the basic energetic range. The comparison of α_p with the experimental results given by Grace (Fig. 3), Cavaleri (Fig. 4) and Massel (Fig. 5) indicates that after spectrum modification, the theoretical coefficient α_p fits the experimental one much better than that before spectrum modification. Thus, the interaction between very low frequency oscillations and wind-induced oscillations plays an important role in the pressure attenuation in the frequency range typical of wind waves. This conclusion can be confirmed more rigorously on the basis of the theory developed above [22]. In addition, it can be demonstrated that the accuracy of the spectral energy estimation in the higher frequencies is of minor importance for the coefficient α_p behaviour.

4. Remarks on the other phenomena influenced on the coefficient α_p

In this chapter we discuss other phenomena which may be important for the pressure attenuation with depth.

i) First we consider the influence of the dispersion relation. The experiments, as well as an analytical solution [21], show that in the high frequency range the dispersion relation is not exactly the classical one-see (2). In general, for the given frequency ω, the resulting wave number k is smaller than that following from (2), *i.e.*:

$$k' < k . \tag{60}$$

Thus, the decaying function (Z) becomes:

$$Z^{(p)'}(\omega_k, z) = \frac{\cosh k'(z+h)}{\cosh k' h} \tag{61}$$

and

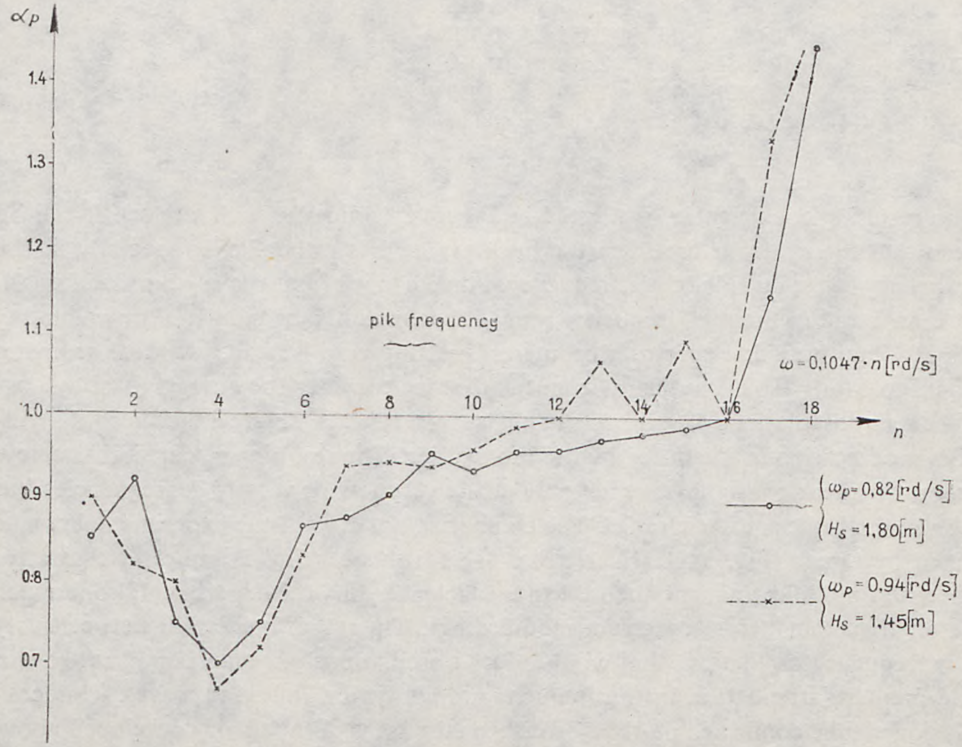

Fig. 5. Empirical coefficient α_p for pore pressure in sandy sea bed, [20]

$$\alpha_p(\omega_k, z) = \frac{Z^{(p)'}(\omega_k, z)}{Z_l^{(p)}(\omega_k, z)} = \frac{\dfrac{\cosh k'(z+h)}{\cosh k' h}}{\dfrac{\cosh k(z+h)}{\cosh \cdot kh}} > 1.0, \tag{62}$$

what is observed exactly in the high frequency range. Moreover, if the dispersion relation influence is considered, two additional problems should be pointed out:
– the second order approximation used in the above theory is insufficient to developed unclassical dispersion relation;

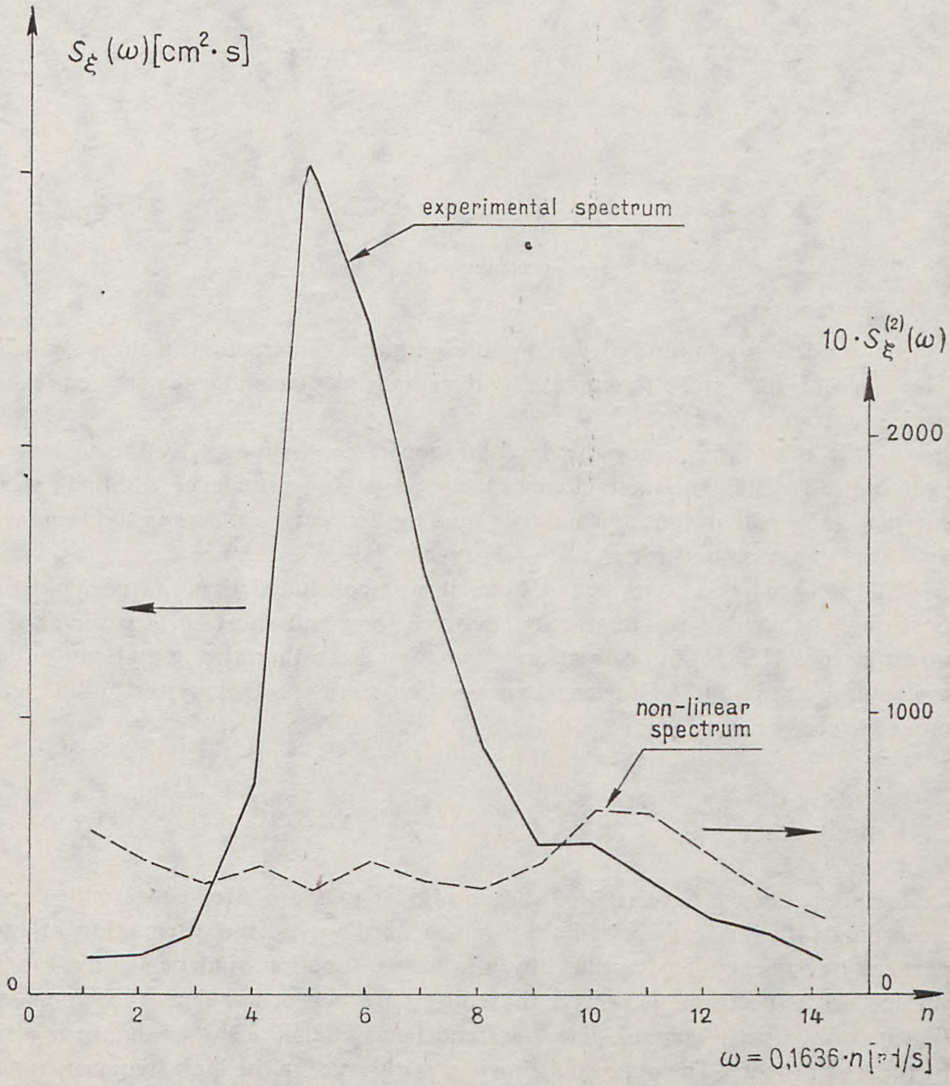

Fig. 6. Separation of the linear and non-linear part of spectrum

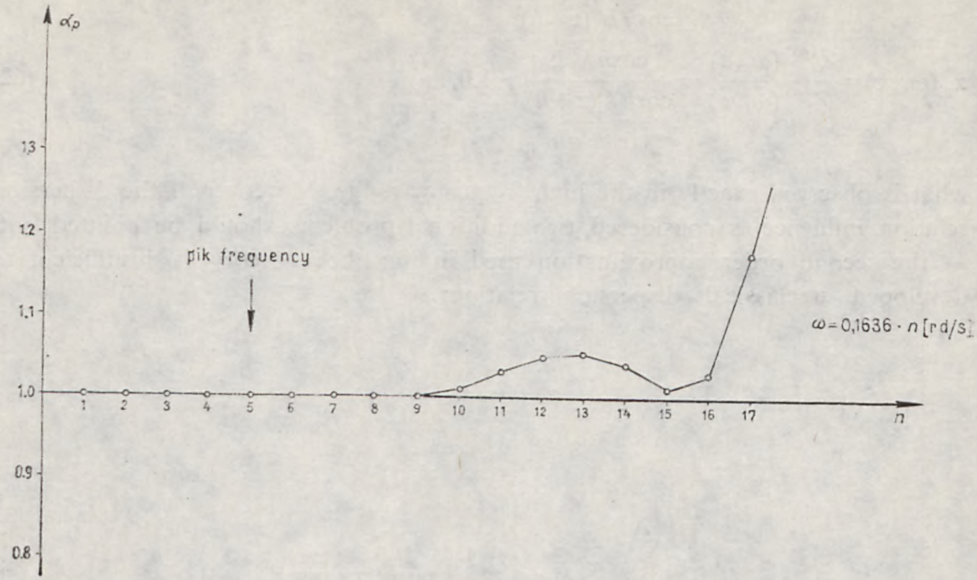

Fig. 7. Attenuation coefficient α_p for spectrum given in Fig. 6

— the dispersion relation reflects also the non-linear interaction in the wave field. Therefore it is impossible to separate (in the simple way) its influence on the pressure decaying from other causes.

ii) In the high frequency the wave motion is contaminated by the turbulence present in the field. The interaction between waves and turbulence, although weak, can play some role in the transmittance function for wave pressure in the same way as it was demonstrated for the orbital velocity [19].

iii) From the results presented here, it was concluded that the coefficient α_p is strongly related to the interaction between long and short surface waves. The investigations [15, 24] indicate clearly that they are rather strong and can not be evaluated by the typical Fourier transformation methods. Usually the WKBJ technique is recommended.

5. Conclusions

In this paper we have studied the non-linear pressure attenuation with depth. According to a linear theory of the wind-induced waves, the attenuation of each particular frequency is described by the same function, independently of the surface wave spectrum. However, the collected experimental data show precisely that it is not true in general. The low frequencies attenuate slower than it is given by the linear theory. The opposite behaviour is observed in the high frequency range.

The analytic method used in chapter 2 offers a theoretical base for understanding this unclassical behaviour. The method employs the perturbation scheme for

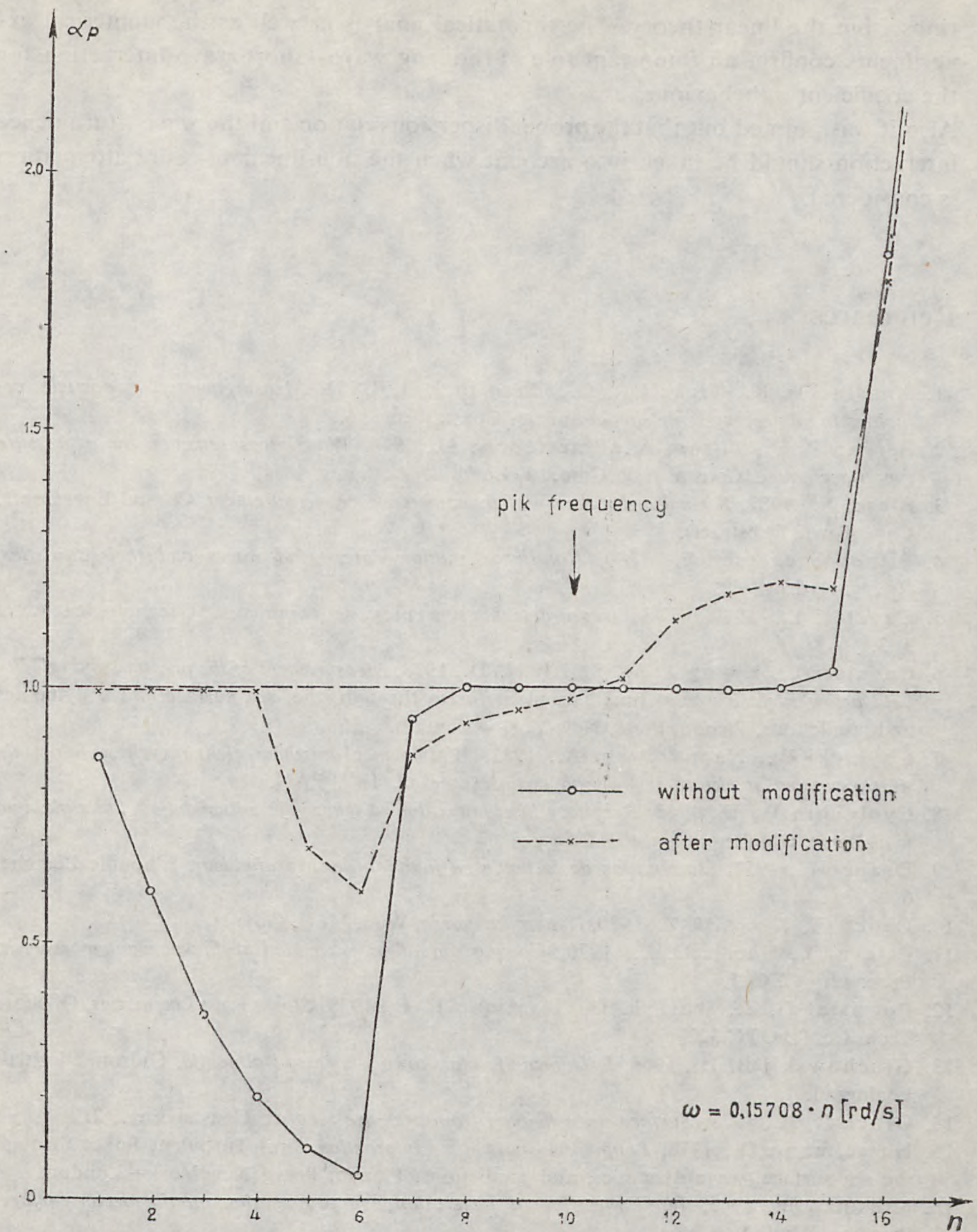

Fig. 8. Influence of the spectrum modification on the coefficient α_p

random surface wave field and the non-linear boundary value problem is solved to the second order, *i.e.* all second order amplitudes and phases are related to the characteristics of the first order spectrum. From the present study it follows that the non-linear interactions generate the additional terms which decay slowly (faster) in the high (low) frequency range and they are responsible for the observed deviations from the linear theory. The theoretical analyis as well as the numerical experiments confirm an important role of the long wave – short wave interaction for the coefficient α_p behaviour.

Also it was pointed out that the proper dispersion relation and the wave – turbulence interaction should be taken into account when the non-linear pressure attenuation is considered.

References

1. Anastasiou K., Tickell R. G., Chaplin J. R., 1982, *Measurements of particle velocities in laboratory-scale random waves*, Coastal Eng., **6**.
2. Bergan P. O., Tørum A., Traetteberg A., 1968, *Wave measurements by a pressure type wave gauge*, Coastal Eng. Conf., **1**, London.
3. Biesel F., 1982, *Second order theory of manometer wave measurement*, Coastal Eng. Conf., Cape Town, (Abstract).
4. Bitner-Gregersen E., 1980, *Non-linear shallow-water wind waves and their statistics*, Rozpr. Hydrot., 42.
5. Cavaleri L., 1980, *Wave measurement using pressure transducer*, Oceanologica Acta, **3**, 3.
6. Cavaleri L., Ewing J. A., Smith N. D., 1978, *Measurement of the pressure and velocity field below surface waves*, [in:] Turbulent fluxes through the sea surface; wave dynamics and predictions, Plenum Press, New York – London.
7. Chybicki W., Naguszewski A., 1983, *Wpływ mechanizmów nieliniowych w falowaniu wiatrowym na strukturę ich widma gęstości energii*, IBW PAN.
8. Cypłuchin W. F., 1963, *Rezultaty instrumentalnowo izuczenija zatuchanija wlon s glubinoj w okieanie*, Okiełanołogija, t. III, 5.
9. Draper L., 1957, *L'atteuation de la houle en function de la profondeur*, L'houille Blanche, 6.
10. Druet C., Kowalik Z., 1970, *Dynamika morza*, Wyd. Mor., Gdynia.
11. Esteva D., Harris D. L., 1970, *Comparison of pressure and staff wave gauge records*, Proc. 12th CEC, **1**.
12. Forristal G. Z., Ward E. G., Borgman L. E., 1978, *Storm wave kinematics*, Offshore Tech. Conf., OTC 3227.
13. Głuchowskij B. H., 1966, *Issledowanije morskowo wietrowo wolnienija*, Gidromietieizdat, Leningrad.
14. Grace R. A., 1978, *Surface wave heights from pressure records*, Coastal Eng., **2**.
15. Hasselmann D., 1978, *Long wave-short wave interaction*, [in:] Turbulent fluxes through the sea surface, wave dynamics, and predictions; Plenum Press, New York – London.
16. Kinsman B., 1965, *Wind waves, their generation and propagation on the ocean surface*, Prentice – Hall, New York.
17. Kryłow J. M., Strekałow S. S., Cypłuchin W. F., 1976, *Wietrowyje wołny i ich wozdziejstwie na sooruzienija*. Gidrometieoizdat., Leningrad.
18. Longuet-Higgins M. S., 1962, *Resonant interaction between two trains of gravity waves*, J. Fluid Mech., **12**,
19. Massel S., 1974, *Kinematyczne charakterystyki falowania wiatrowego*, Oceanol., 3.
20. Massel S., 1982, *Rozklad ciśnień parowych wywolanych falowaniem wiatrowym w piaszczystej warstwie dna morskiego*, Rozpr. Hydrot., 44.
21. Massel S., Chybicki W., 1983, *Związek dyspersyjny dla fal wiatrowych, Analiza nieliniowa*, Stud. i Mater. Oceanogr., 40.

22. Naguszewski A., Massel S., Trapp W., 1983, *Zanikanie falowania wodnego wzbudzanego wiatrem w głąb akwenu. Wpływ nieliniowości ruchu*, IBW PAN, Gdańsk.
23. Ohmart R. D., Gratz R. L., 1978, *Comparison of measured and predicted ocean wave kinematics*, Offshore Techn. Conf., OTC 3276.
24. Phillips O. M., 1977, *The dynamics of upper ocean*, Acad. Press, London.
25. Sharma J. N., Dean R. G., 1981, *Second-order directional seas and associated wave forces*, Soc. of Petr. Eng. J.
26. Tick L. J., 1959, *A non-linear random model of gravity waves*, J. Math. and Mech., **8**, 5.
27. Vis F. C., 1980, *Oribital velocities in irregular waves*, Coastal Eng. Conf., **1**.
28. Wehausen J. V., Laitone E. V., *Surface waves*, [in:] Encyclopedia of Physics, **IX**, Springer-Verlag.